K. Singh[1], I. Kaur[2]

MODIFIED MOORE-GIBSON-THOMPSON THERMOELASTIC MODEL WITH TWO TEMPERATURES EFFECT ON ROTATING SEMICONDUCTING THERMOELASTIC SOLID CYLINDER

[1]*Faculty of Engineering, UIET, Kurukshetra University, Haryana, India*
[2]*Department of Mathematics, Government College for Girls, Palwal, Kurukshetra, India*
e-mail: 1ksingh2015@kuk.ac.in

Abstract. A rotating semiconducting cylinder is studied within the framework of photo-thermoelasticity. The cylinder is exposed to an exponential pulse, acting as a variable heat flux. The study utilizes the Moore-Gibson-Thompson-Photo-Thermal equations of heat transfer. They incorporate two temperatures to describe the basic equations of the system. The Laplace transform is employed which allows for a more efficient and accurate solution. To calculate the displacement components, carrier density, thermal stresses, and conductive temperature in the physical domain, the numerical inversion techniques are utilized. Furthermore, MATLAB software is employed to generate graphical representations of all the parameters involved in the study. These visualizations illustrate the impact of thermal relaxations and various thermoelasticity theories that consider two temperatures.

Keywords: semiconducting cylinder, two temperature, modified Moore-Gibson-Thompson heat transfer, exponential pulse.

1. Introduction.

Semiconductor materials have garnered significant attention in recent years owing to their unique physical properties. At room temperature, semiconductor materials do not show good conductivity, in comparison with metals like copper or aluminum. Furthermore, they do not possess the insulating properties of materials like glass. However, as the temperature rises, the semiconductor materials resistance gradually decreases, leading to enhanced electrical conductivity. This characteristic has made semiconductor materials indispensable in modern VLSI, and electrical industries. When semiconductor materials are heated, their physical properties are altered as a result of deformation. Two primary types of deformation occur as a result of thermal effects: thermoelastic deformation and electronic deformation. Thermoelastic deformation is observed when semiconductor materials are subjected to focused laser or sunlight beams, causing them to vibrate. The semiconductor materials can be found in a wide range of applications in renewable energy, especially solar cell technology, where they make it possible to harness solar energy efficiently.

In 1938, Duhamel [1] introduced an uncoupled classical theory of thermoelasticity. However, this theory had two limitations. Firstly, it did not consider the relationship between the material's state and its temperature. Secondly, the parabolic heat equations predicted that temperature could travel at an infinite speed, which contradicted experimental observations. To address these limitations, Biot [2] proposed a coupled thermoelasticity theory that explained the connection between elasticity and heat conduction equations. However, this theory had the drawback of only predicting heat waves with unlimited propagation speeds. To overcome this, Vernotte [4, 5] and Cattaneo [3] suggested incorporating a relaxation time into the heat flux vector in relation to the temperature gradient. This modification aimed to achieve a steady state when there is an abrupt change in temperature in a homogeneous and isotropic medium as:

$$\left(1+\tau_0 \frac{\partial}{\partial t}\right) q = -K_{ij} \partial T. \tag{1}$$

After that, Lord and Shulman [6] introduced a generalized theory of thermoelasticity for an isotropic body with one relaxation time, which states that due to the hyperbolic nature of the heat equation, temperature propagates at a finite speed. This theory provided a significant advancement in understanding the behavior of heat in materials. The knowledge of thermoelasticity was further improved by Chen and Gurtin [7] by combining the two concepts of thermodynamic temperature – which is generated by mechanical processes – and conductive temperature, resulting from thermodynamic processes. This more precise version of thermoelasticity allowed for a comprehensive analysis of the temperature distribution in materials. Green and Lindsay [8] presented a symmetrical linear heat conduction tensor, which played a crucial role in the development of thermoelasticity. This tensor provided a mathematical framework to describe the conduction of heat in materials, enabling a deeper understanding of the underlying mechanisms. Dhaliwal and Sherief [9] extended the equations of generalized thermoelasticity to anisotropic media. Their contributions allowed for a more comprehensive analysis of materials with varying properties in different directions, providing a more accurate representation of real-world scenarios.

Green and Naghdi [10 – 12] made significant helps to the field of thermoelasticity by further advancing the theories with and without energy dissipation. Their work not only improved the understanding of heat conduction but also enhanced the Fourier law, which describes the relationship between heat flux and temperature gradient in materials as:

$$q = -K_{ij} \nabla \mathrm{T} - K_{ij}^{*} \nabla \vartheta; \;\; \dot{\vartheta} = T; \;\; T = \varphi - a_{ij} \varphi_{,ij}. \tag{2}$$

This 3rd-order differential equation plays a crucial role in specific fluid dynamics and serves as the foundation for Lasiecka and Wang's theory [13], as referenced in their work. Quintanilla [14, 15], in his research, introduced a novel model of heat conduction by incorporating the MGT equation with 2T, further solidifying the equation's importance in the field. Referred to as the modified Fourier law, the MGT equation continues to be a focal point for researchers exploring various applications and implications within the realm of fluid dynamics and heat conduction.

$$\left(1+\tau_0 \frac{\partial}{\partial t}\right) \boldsymbol{q} = -K_{ij} \nabla \boldsymbol{T} - K_{ij}^{*} \nabla \vartheta, \text{ where, } \dot{\vartheta} = \boldsymbol{T}. \tag{3}$$

Fernandez and Quintanilla [16] explored the topic of linear thermoelastic distortions in dielectrics, while Bazarra et al [17] delved into a thermoelastic issue using the MGT thermoelastic equation. In the context of semiconductor elastic media, the excitation of free electrons by external laser beams leads to a significant increase in the density of charge carriers at a low semiconductor gap energy E_g. This, in turn, triggers electronic deformations and elastic vibrations as a response to absorbed optical radiation. Consequently, the presence of thermoelastic plasma waves becomes a crucial factor in determining heat conductivity calculations.

A generalized formulation of the updated Fourier law for SM materials, taking into account the influence of plasma, can be derived as

$$\left(1+\tau_0 \frac{\partial}{\partial t}\right) \boldsymbol{q} = -K_{ij} \nabla \boldsymbol{T} - K_{ij}^{*} \nabla \vartheta - \int \frac{E_g \boldsymbol{N}}{\tau} d\boldsymbol{x}, \text{ where, } \dot{\vartheta} = \boldsymbol{T}. \tag{4}$$

Photo-excitation is represented by the last term in Eq. (4). Differentiating equation (4) w.r.t. x, yields

$$\left(1+\tau_0\frac{\partial}{\partial t}\right)\nabla\cdot\boldsymbol{q}=-\nabla\cdot\left(K_{ij}\nabla\boldsymbol{T}+K_{ij}^{*}\nabla\vartheta\right)-\frac{E_g\boldsymbol{N}}{\tau},\ \text{where, } \dot{\vartheta}=\boldsymbol{T}. \tag{5}$$

Several other researchers, including Kaur et al. [18, 19], Lata et al. [20], Kaur and Singh [21 – 23], Kaur et al. [24], Singh et al. [25], have also conducted similar studies on semiconductor media. However, there is a lack of research on the transient research of semiconductor cylinders with two temperatures exposed to photo-generated plasma and ultras-hort pulsed laser heating, as revealed by the literature review. By reviewing the significance of the problem in depth, the study intends to address this gap.

2. Basic Equations.

The constitutive equations [26, 27] for an MGTPT with thermal-plasma-elastic interaction are given by:

I. Constitutive relations

$$\sigma_{ij}=\left(\lambda u_{k,k}-\beta T-\delta_n N\right)\delta_{ij}+\mu\left(u_{i,j}+u_{j,i}\right);$$
$$\beta=\left(3\lambda+2\mu\right)\alpha_t;\ \delta_n=\left(3\lambda+2\mu\right)d_n;\ T=\varphi-a_{ij}\varphi_{,ij}. \tag{6}$$

II. Equation of motion

$$\sigma_{ij,j}+F_i=\rho\left\{\ddot{u}_i+\Omega\times\left(\Omega\times u\right)+2\Omega\times\dot{u}\right\}, \tag{7}$$

where, $\Omega\times(\Omega\times u)$ and $2\Omega\times\dot{u}$ are the centripetal acceleration and Coriolis acceleration.

III. Plasma diffusion equation

$$\frac{\partial\boldsymbol{N}}{\partial t}=D_E\nabla^2\boldsymbol{N}-\frac{\boldsymbol{N}}{\tau}+\kappa\left(1-a\nabla^2\right)\varphi,\ \text{where, } \kappa=\frac{T}{\tau}\frac{\partial N_0}{\partial T}. \tag{8}$$

IV. Modified MGT heat conduction equation

$$\left(K_{ij}\dot{\varphi}_{,j}\right)_{,i}+\left(K_{ij}^{*}\varphi_{,j}\right)_{,i}+\frac{E_g\dot{\boldsymbol{N}}}{\tau}=\left(1+\tau_0\frac{\partial}{\partial t}\right)\left[\rho C_E\left(1-a\nabla^2\right)\ddot{\varphi}+\beta_{ij}T_0\ddot{e}_{ij}-\rho\dot{Q}\right], \tag{9}$$

where, $K_{ij}=K_i\delta_{ij}$, $K_{ij}^{*}=K_i^{*}\delta_{ij}$, i is not summed.

Also, the subscript followed ‘,’ a comma denotes the partsal derivative w.r.t. spase coordinates and a superposed ‘.’ signifies differentiation w.r.t. variable, where

$$\epsilon_{ijk}=\epsilon_{jki}=\epsilon_{kij}=-\epsilon_{jik}=-\epsilon_{kji}=-\epsilon_{ikj};$$

$$\epsilon_{ijk}=\begin{cases}+1,\ \mathit{if}\ (i,j,k)\ \text{is even permutation of } (1,2,3);\\ -1,\ \mathit{if}\ (i,j,k)\ \text{is odd permutation of } (1,2,3);\\ \quad 0,\quad \text{if two or more indices are equal}\end{cases}$$

$$\left(Eg, \epsilon_{123}=+1, \epsilon_{132}=-1, \epsilon_{122}=0\right).$$

3. Method and solution of the problem.

Consider a semiconductor solid cylinder with symmetric and thermally homogeneous properties, having a radius of r_0. Laser pulses from an external heating device have been used to heat the exterior of the cylinder. The cylindrical coordinate system (r,θ,z) is aligned with the z-axis parallel to the cylinder axis, while the cylinder starts at a constant and uniform temperature of (T_0).

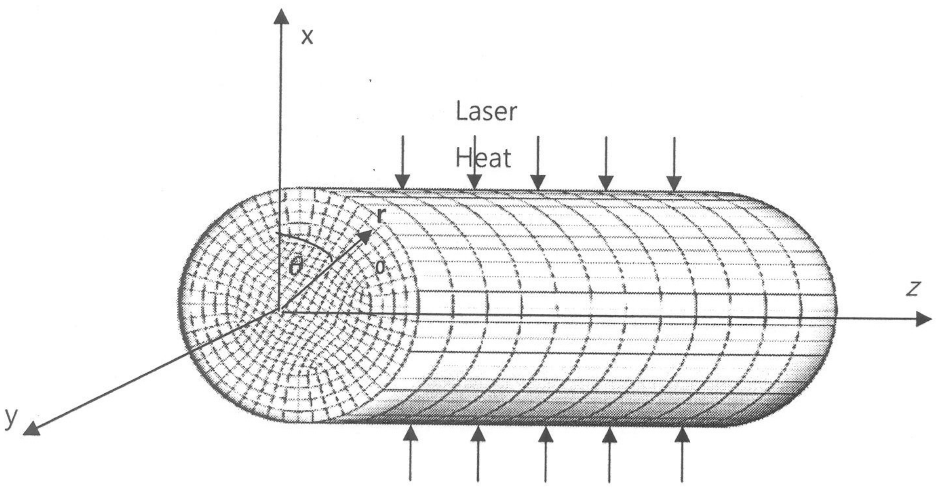

Fig. 1. Structure of problem.

Furthermore, in order to meet the regularity criterion, it is presupposed that each field being examined is finite within the given medium. The functions being considered are affected by both the radial distance r and the time t in the case of a 1-D problem, owing to its symmetry. The expressions for displacement-strain and displacement components are formulated accordingly.

$$\boldsymbol{u}=\left(u,0,0\right)\left(r,t\right);$$
$$e_{rr}=\frac{u}{r};\ e_{\theta\theta}=\frac{\partial u}{\partial r};\ e_{r\theta}=e_{rz}=e_{\theta z}=e_{zz}=0. \tag{10}$$

The equation (5) using (8) will be the form

$$\sigma_{rr}=2\mu\frac{\partial u}{\partial r}+\lambda e-\left(\beta(1-a\nabla^2)\varphi+\delta_n N\right); \tag{11}$$

$$\sigma_{\theta\theta}=2\mu\frac{u}{r}+\lambda e-\left(\beta(1-a\nabla)^2\varphi+\delta_n N\right); \tag{12}$$

$$\sigma_{zz}=\lambda e-\left(\beta(1-a\nabla^2)\varphi+\delta_n N\right); \tag{13}$$

$$\nabla^2=\frac{\partial^2}{\partial r^2}+\frac{1}{r}\frac{\partial}{\partial r};\quad e_{kk}=e=\frac{1}{r}\frac{\partial\left(ru\right)}{\partial r}.$$

Hence, the dynamic motion equation becomes

$$\frac{\partial\sigma_{rr}}{\partial r}+\frac{1}{r}\left(\sigma_{rr}-\sigma_{\theta\theta}\right)=\rho\left(\frac{\partial^2 u}{\partial t^2}-\Omega^2 u\right). \tag{14}$$

Using equations (11) – (13), in equations (14) and (8) – (9), yields:

$$\left(\lambda+2\mu\right)\frac{\partial}{\partial r}\left(\frac{1}{r}\frac{\partial\left(ru\right)}{\partial r}\right)-\beta\frac{\partial}{\partial r}\left\{\left(1-a\nabla^2\right)\varphi\right\}-\delta_n\frac{\partial N}{\partial r}=\rho\left(\frac{\partial^2 u}{\partial t^2}\right); \tag{15}$$

$$\frac{\partial N}{\partial t}=D_E\left(\nabla^2 N\right)-\frac{N}{\tau}+\kappa\left(1-a\nabla^2\right)\varphi; \tag{16}$$

$$K\frac{\partial}{\partial t}\nabla^2\varphi + K^*\nabla^2\varphi + \frac{E_g\dot{N}}{\tau} = \left(1+\tau_0\frac{\partial}{\partial t}\right)\left[\rho C_E\frac{\partial^2}{\partial t^2}\left\{\left(1-a\nabla^2\right)\varphi\right\} + \beta T_0\frac{\partial^2 e}{\partial t^2}\right]. \quad (17)$$

Pre-operating both sides of Eq. (15) by $\left(1/r + \partial/\partial r\right)$, we obtain

$$\left(\lambda+2\mu\right)\nabla^2 e - \beta\nabla^2\left(1-a\nabla^2\right)\varphi - \delta_n\nabla^2 N = \left(\frac{\partial^2 e}{\partial t^2}\right). \quad (18)$$

The aforementioned equations can be transformed into dimensionless form using the following dimensionless quantities:

$$\begin{gathered}(r',u') = v_0\eta\left(r,u\right);\ \left(T',N',\sigma'_{ij},\varphi'\right) = \frac{1}{\rho v_0^2}\left(\beta T,\delta_n N,\sigma_{ij},\varphi\right);\\ (\tau_0',\tau',t') = v_0^2\eta(\tau_0,\tau,t);\ \eta = \frac{\rho C_E}{K};\ \rho v_0^2 = \lambda+2\mu;\ \gamma = \sqrt{\frac{\mu}{\lambda+2\mu}}.\end{gathered} \quad (19)$$

The magnetic parameter M (sometimes referred to as the Hartmann number) determines the magnetic field's strength in this instance. After suppressing the primes, applying (19) to equations (15) – (17) yields

$$\nabla^2 e - \nabla^2\left(1-a\nabla^2\right)\varphi - \nabla^2 N = \left(\frac{\partial^2 e}{\partial t^2}\right); \quad (20)$$

$$\frac{\partial N}{\partial t} = \delta_1(\nabla^2 N) - \delta_2 N + \delta_3(1-a\nabla^2)\varphi; \quad (21)$$

$$\frac{\partial}{\partial t}\nabla^2\varphi + \delta_4\nabla^2\varphi + \delta_5 N = \left(1+\tau_0\frac{\partial}{\partial t}\right)\left[\frac{\partial^2}{\partial t^2}\left(1-a\nabla^2\right)\varphi + \delta_6\frac{\partial^2 e}{\partial t^2}\right], \quad (22)$$

where,

$$\begin{gathered}\delta_1 = D_E\eta;\ \delta_2 = \frac{1}{\tau};\ \delta_3 = \frac{\kappa\delta_n}{\beta};\ \delta_4 = \frac{K^*}{\left(\lambda+2\mu\right)C_E};\\ \delta_5 = \frac{E_g}{\delta_n C_E\left(\lambda+2\mu\right)\eta\tau};\ \delta_6 = \frac{\beta^2 T_0}{\rho C_E\left(\lambda+2\mu\right)}.\end{gathered} \quad (23)$$

Using equation (19) in equations (11) – (13) and after suppressing the primes, yields

$$\sigma_{rr} = 2\gamma^2\frac{\partial u}{\partial r} + (1-2\gamma^2)e - \left((1-a\nabla^2)\varphi + N\right); \quad (24)$$

$$\sigma_{\theta\theta} = 2\gamma^2\frac{u}{r} + (1-2\gamma^2)e - \left((1-a\nabla^2)\varphi + N\right); \quad (25)$$

$$\sigma_{zz} = (1-2\gamma^2)e - \left((1-a\nabla^2)\varphi + N\right). \quad (26)$$

Initial conditions are assumed as

$$u\left(r,0\right) = 0 = \frac{\partial u}{\partial r}\left(r,0\right); \quad (27)$$

$$\varphi\left(r,0\right) = 0 = \frac{\partial\varphi}{\partial r}\left(r,0\right); \quad (28)$$

$$N\left(r,0\right) = 0 = \frac{\partial N}{\partial r}\left(r,0\right). \quad (29)$$

The Laplace transform of a function f w.r.t. time variable t, is defined as

$$\mathcal{L}\left(f\left(t\right)\right)=\overline{f}\left(s\right)=\int\limits_{0}^{\infty}f\left(t\right)e^{-st}dt. \tag{30}$$

Using Laplace transforms from Eq. (30) to (20) – (22) yields

$$\left(\nabla^2+\Omega^2-s^2\right)\overline{e}-\nabla^2\left(1-a\nabla^2\right)\overline{\varphi}-\nabla^2\overline{N}=0; \tag{31}$$

$$\left(\delta_1\nabla^2-\left(\delta_2+s\right)\right)\overline{N}+\delta_3\left(1-a\nabla^2\right)\overline{\varphi}=0; \tag{32}$$

$$\left(1+\tau_0 s\right)\delta_6 s^2\overline{e}+\left(-\left(s+\delta_4\right)\nabla^2+\left(1+\tau_0 s\right)s^2\left(1-a\nabla^2\right)\right)\overline{\varphi}-\delta_5\overline{N}=0. \tag{33}$$

Using Laplace transforms on equations (30) to equations (24) – (26), we obtain

$$\overline{\sigma_{rr}}=2\gamma^2\frac{\partial\overline{u}}{\partial r}+\left(1-2\gamma^2\right)\overline{e}-\left(\left(1-a\nabla^2\right)\overline{\varphi}+\overline{N}\right); \tag{34}$$

$$\overline{\sigma_{\theta\theta}}=2\gamma^2\frac{\overline{u}}{r}+\left(1-2\gamma^2\right)\overline{e}-\left(\left(1-a\nabla^2\right)\overline{\varphi}+\overline{N}\right); \tag{35}$$

$$\overline{\sigma_{zz}}=\left(1-2\gamma^2\right)\overline{e}-\left(\left(1-a\nabla^2\right)\overline{\varphi}+\overline{N}\right). \tag{36}$$

When Eq. (31) to (33) are decoupled, we get

$$\left(\nabla^6-B\nabla^4+C\nabla^2-D\right)\left(\overline{e},\overline{\varphi},\overline{N}\right)=0, \tag{37}$$

where,

$$A=-\delta_1\delta_{11};$$

$$B=-\left(a\delta_3\delta_5 s+-A\delta_7-\delta_1\delta_{10}-\delta_1\delta_9+\delta_8\delta_{11}-a\delta_8\delta_9\right)/A;$$

$$C=\left(-\delta_3\delta_5 s+a\delta_3\delta_5\delta_7+\delta_3\delta_9-\delta_1\delta_7\delta_{10}+\delta_8\delta_7\delta_{11}+\delta_8\delta_{10}+\delta_8\delta_9\right)/A;$$

$$D=\left(\delta_3\delta_7\delta_5 s-\delta_8\delta_7\delta_{10}\right)/A;$$

$$\delta_7=\left(\Omega^2-s^2\right);\ \delta_8=\delta_2+s;\ \delta_9=\left(1+\tau_0 s\right)\delta_6 s^2;$$

$$\delta_{10}=\left(1+\tau_0 s\right)s^2;\ \delta_{11}=-\left(s+\delta_4\right)-\left(1+\tau_0 s\right)s^2 a.$$

Presenting $\lambda_i, i=1,2,3,$ in equations (37), we obtain

$$\left(\nabla^2-\lambda_1^2\right)\left(\nabla^2-\lambda_2^2\right)\left(\nabla^2-\lambda_3^2\right)\left(\overline{e},\overline{\varphi},\overline{N}\right)=0, \tag{38}$$

where, $\lambda_i^2, i=1,2,3,$ are the roots of the equation

$$\left(\lambda^6-B\lambda^4+C\lambda^2-D\right)=0.$$

Which are given by

$$\lambda_1^2=\frac{1}{3}\left(2\omega\sin\xi+B\right); \tag{39}$$

$$\lambda_2^2=\frac{1}{3}\left(-\omega\sin\xi-\sqrt{3}\omega\cos\xi+B\right); \tag{40}$$

$$\lambda_3^2=\frac{1}{3}\left(-\omega\sin\xi+\sqrt{3}\omega\cos\xi+B\right). \tag{41}$$

With

$$\omega = \sqrt{B^2 - 3C};\ \xi = \frac{1}{3}\sin^{-1}\left(-\frac{2B^3 - 9BC + 27D}{2\omega^3}\right).$$

The solution to Equation (38) can be expressed in a general form as

$$\left(\overline{e}, \overline{\varphi}, \overline{N}\right) = \sum_{i=1}^{3}\left(1, \zeta_i, \eta_i\right) g_i I_0\left(\lambda_i r\right), \tag{42}$$

where $I_n(\ )$ represents the second form of n^{th} order modified Bessel functions. We obtain the following terms by using Eq. (42) into Eqs. (31) to (33)

$$\zeta_i = \frac{-\left(\lambda_i^2 + \delta_7\right)\left(\delta_9\lambda_i^2 - \delta_5\right)}{\delta_3\delta_5 + \left(\delta_{11}\lambda_i^2 + \delta_{10}\right)\left(\delta_1\lambda_i^2 - \delta_8\right)}; \tag{43}$$

$$\eta_i = \frac{-(\lambda_i^2 + \delta_7)(\delta_3)}{\delta_3\delta_5 + (\delta_{11}\lambda_i^2 + \delta_{10})(\delta_1\lambda_i^2 - \delta_8)}. \tag{44}$$

Within the realm of the Laplace transform, the variable representing displacement u, can be articulated in a subsequent manner:

$$\overline{u} = \sum_{i=1}^{3}\frac{1}{\lambda_i} g_i I_1\left(\lambda_i r\right). \tag{45}$$

We obtained Eq. (45) using Bessel function relation

$$\int x I_0(x)dx = x I_1(x). \tag{46}$$

Differentiating Equation (45) in terms of r yields

$$\frac{\partial \overline{u}}{\partial r} = \sum_{i=1}^{3} g_i\left[I_0\left(\lambda_i r\right) - \frac{1}{\lambda_i r} I_1\left(\lambda_i r\right)\right]. \tag{47}$$

Consequently, the closed-form expression for thermal stress is derived as:

$$\overline{\sigma_{rr}} = \sum_{i=1}^{3} g_i\left\{l_i I_0\left(\lambda_i r\right) - \frac{2\gamma^2}{\lambda_i r} I_1\left(\lambda_i r\right)\right\}; \tag{48}$$

$$\overline{\sigma_{\theta\theta}} = \sum_{i=1}^{3} g_i\left\{\frac{2\gamma^2}{\lambda_i r} I_1\left(\lambda_i r\right) + l_i I_0\left(\lambda_i r\right)\right\}; \tag{49}$$

$$\overline{\sigma_{zz}} = \sum_{i=1}^{3} g_i l_i I_0\left(\lambda_i r\right); \tag{50}$$

$$l_i = 1 - 2\gamma^2 - \left(\zeta_i(1 - a\lambda_i^2) + \eta_i\right).$$

4. Boundary conditions.

It is hypothesized that an external force is acting upon the outer surface of the cylinder. As a result of this force, the mechanical boundary condition can be expressed as

$$1 - a\lambda_i^2. \tag{51}$$

Furthermore, a variable heat flux, specifically exponentially pulsed laser heat, is applied at the periphery of the cylinder. This results in the establishment of certain boundary conditions that need to be taken into consideration when analyzing the system as

$$q_p = q_0 \frac{t^2}{16t_p^2} e^{-t/t_p}; \quad \text{at } r = r_0. \tag{52}$$

Using (32) in equation (3) yields

$$\left(1 + \tau_0 \frac{\partial}{\partial t}\right) \dot{q}_p = -\left(\frac{\partial}{\partial t} + \delta_4\right) \frac{\partial T}{\partial r}, \tag{53}$$

Equations (52) and (53) yields the subsequent boundary condition

$$\frac{q_0}{16t_p^2} \left(1 + \tau_0 \frac{\partial}{\partial t}\right) \frac{\partial}{\partial t} \left(t^2 e^{-t/t_p}\right) = -\left(\frac{\partial}{\partial t} + \delta_4\right) \frac{\partial T}{\partial r}, \text{ at } r = r_0. \tag{54}$$

During the diffusion phase, carriers have the ability to come into contact with the sample surface, where there exists a certain likelihood of recombination taking place. The boundary conditions for carrier density are as follows:

$$D_E \frac{\partial N}{\partial r} = s_v N, \text{ at } r = r_0. \tag{55}$$

By applying Laplace transform on the boundary conditions (51), (54), and (55) yield

$$\bar{u}\left(r_0, s\right) = 0; \tag{56}$$

$$\left.\frac{\partial (1 - a\nabla^2)\bar{\varphi}}{\partial r}\right|_{r=r_0} = -\frac{q_0 (1 + \tau_0 s) s}{8(1 + s t_p)^3 (s + \delta_4)} = -\bar{G}\left(s\right); \tag{57}$$

$$D_E \left.\frac{\partial \bar{N}}{\partial r}\right|_{r=r_0} = s_v \bar{N}\left(r_0, s\right). \tag{58}$$

Equations (42) and (45) are substituted into Eq. (56) – (58), giving

$$\sum_{i=1}^{3} g_i \frac{1}{\lambda_i} I_1\left(\lambda_i r_0\right) = 0; \tag{59}$$

$$\sum_{i=1}^{3} g_i I_1\left(\lambda_i r_0\right) \zeta_i \lambda_i (1 - a\lambda_i^2) = -\frac{q_0\left(1 + \tau_0 s\right) s t_p}{8(1 + s t_p)^3 (s + \delta_4)} = -\bar{G}\left(s\right); \tag{60}$$

$$\sum_{i=1}^{3} \eta_i g_i \left\{ D_E \lambda_i I_1\left(\lambda_i r_0\right) - s_v I_0\left(\lambda_i r_0\right) \right\} = 0. \tag{61}$$

Solving equations (59) – (61) using Cramer's rule, we can get the values of $g_i, i = 1,2,3$

$$g_i\left(s\right) = \frac{\Delta_i}{\Delta};$$

$$\Delta = \mathrm{G}_1\left[\mathrm{G}_5\mathrm{G}_9 - \mathrm{G}_8\mathrm{G}_6\right] - \mathrm{G}_2\left[\mathrm{G}_4\mathrm{G}_9 - \mathrm{G}_6\mathrm{G}_7\right] + \mathrm{G}_3\left[\mathrm{G}_4\mathrm{G}_8 - \mathrm{G}_5\mathrm{G}_7\right];$$

$$\Delta_1 = \bar{G}\left(s\right)\left[\mathrm{G}_2\mathrm{G}_9 - \mathrm{G}_8\mathrm{G}_3\right]; \; \Delta_2 = \bar{G}\left(s\right)\left[\mathrm{G}_1\mathrm{G}_9 - \mathrm{G}_7\mathrm{G}_3\right]; \; \Delta_3 = \bar{G}\left(s\right)\left[\mathrm{G}_1\mathrm{G}_8 - \mathrm{G}_2\mathrm{G}_7\right];$$

$$\mathrm{G}_{\mathrm{i}} = \frac{1}{\lambda_i}\phi_i; \; \mathrm{G}_{\mathrm{i+3}} = \phi_i \zeta_i \lambda_i \left(1 - a\lambda_i^2\right); \; \mathrm{G}_{\mathrm{i+6}} = \eta_i \left\{ D_E \lambda_i \phi_i - s_v \psi_i \right\};$$

$$I_1\left(\lambda_i r_0\right) = \phi_i; \; I_0\left(\lambda_i r_0\right) = \psi_i, \quad i = 1,2,3.$$

and by using the values of $g_i(s)$ in (42), (45), (48) – (50), the expression for displacement, temperature distribution, carrier density, and stresses can be obtained as:

$$\bar{u} = \frac{\bar{G}(s)}{\Delta}\left\{[G_2G_9 - G_8G_3]\frac{\theta_1}{\lambda_1} - [G_1G_9 - G_7G_3]\frac{\theta_2}{\lambda_2} + [G_1G_8 - G_2G_7]\frac{\theta_3}{\lambda_3}\right\}; \tag{62}$$

$$\bar{T} = \frac{\bar{G}(s)}{\Delta}\left\{[G_2G_9 - G_8G_3]\zeta_1\vartheta_1 - [G_1G_9 - G_7G_3]\zeta_2\vartheta_2 + [G_1G_8 - G_2G_7]\zeta_3\vartheta_3\right\}; \tag{63}$$

$$\bar{N} = \frac{\bar{G}(s)}{\Delta}\left\{[G_2G_9 - G_8G_3]\eta_1\vartheta_1 - [G_1G_9 - G_7G_3]\eta_2\vartheta_2 + [G_1G_8 - G_2G_7]\eta_3\vartheta_3\right\}; \tag{64}$$

$$\overline{\sigma_{rr}} = \frac{\bar{G}(s)}{\Delta}\left\{\begin{array}{c}[G_2G_9 - G_8G_3](l_1\vartheta_1 - \mu_1) - [G_1G_9 - G_7G_3](l_2\vartheta_2 - \mu_2) + \\ +[G_1G_8 - G_2G_7](l_3\vartheta_3 - \mu_3)\end{array}\right\}; \tag{65}$$

$$\overline{\sigma_{\theta\theta}} = \frac{\bar{G}(s)}{\Delta}\left\{\begin{array}{c}[G_2G_9 - G_8G_3]\{\mu_1 + l_1\vartheta_1\} - [G_1G_9 - G_7G_3]\{\mu_2 + l_2\vartheta_2\} + \\ +[G_1G_8 - G_2G_7]\{\mu_3 + l_3\vartheta_3\}\end{array}\right\}; \tag{66}$$

$$\overline{\sigma_{zz}} = \frac{\bar{G}(s)}{\Delta}\left\{\begin{array}{c}[G_2G_9 - G_8G_3]l_1\vartheta_1 - [G_1G_9 - G_7G_3]l_2\vartheta_2 + \\ +[G_1G_8 - G_2G_7]l_3\vartheta_3\end{array}\right\}, \tag{67}$$

where

$$\vartheta_i = I_0(\lambda_i r);\ \theta_i = I_1(\lambda_i r);\ \mu_i = \frac{2\gamma^2}{\lambda_i r} I_1(\lambda_i r),\quad i = 1,2,3.$$

5. Inversion of the transforms.

The method to find the solution within the physical domain involves the process of inverting the transforms specified in equations (62) – (67) using

$$f(x,t) = \frac{1}{2\pi i}\int_{e^{-i\infty}}^{e^{+i\infty}} \tilde{f}(x,s)e^{-st}ds. \tag{68}$$

To calculate the integral in equation (68), it is recommended to utilize Romberg's integration method with adaptive step size, as suggested by Press et al. [28] in their work.

6. Particular cases.

If $K^* \neq 0, K \neq 0$ and $\tau_0 \neq 0, a \neq 0$ in equation (62) – (67), it is possible to acquire the outcomes of the MGTPT+2TT.

If $K^* \neq 0, K \neq 0$ and $\tau_0 = 0, a \neq 0$ in equation (62) – (67), the outcomes of the PGN-III model, which incorporates two temperatures, are obtainable.

If $K \neq 0$ and $\tau_0 = 0, a \neq 0$ in equation (62) – (67), the results of photothermal Green – Naghdi II model (PGN-II) with two temperatures can be acquired.

If $\tau_0 = 0,\ K^* = 0,\ a \neq 0$ in equation (62) – (67), the results of coupled photo-thermoelasticity theory (CPTE) with two temperatures are achieved.

If $K^* = 0,\ a \neq 0$, in equation (62) – (67), the outcomes of the generalized Lord and Shulman photo-thermoelasticity model (PLS) with two temperatures are achieved.

If $a = 0$ in equation (62) – (67), the outcomes of MGTPT model is achieved.

7. Numerical results and discussion.

MATLAB software is utilized to visually represent the impact of two different temperatures and the MGTPT on silicon (Si) material. The theoretical findings are supported by the physical data of silicon. This approach allows for a broad understanding of the effects and behavior of silicon under varying temperature conditions, providing valuable insights into its characteristics and performance.

$$\lambda = 3{,}64\times10^{10}\,\mathrm{Nm^{-2}};\ \mathrm{T_0} = 300\ \mathrm{K};\ \mu = 5{,}46\times10^{10}\,\mathrm{Nm^{-2}};\ \mathrm{H_0} = 1\ \mathrm{Jm^{-1}nb^{-1}};$$

$$\beta = 7{,}04\times10^{6}\,\mathrm{Nm^{-2}deg^{-1}};\ \tau = 5\times10^{-5}\,\mathrm{s};\ \delta_n = -9\times10^{-31}\,\mathrm{m^{-3}};\ N_0 = 10^{20}\,\mathrm{m^{-3}};$$

$$\rho = 2{,}33\times10^{3}\,\mathrm{kgm^{-3}};\ \varepsilon_0 = 8{,}838\times10^{-12}\,\mathrm{Fm^{-1}};\ C_E = 695\,\mathrm{Jkg^{-1}K^{-1}};\ E_g = 1{,}11\mathrm{eV};$$

$$K = 150\,\mathrm{Wm^{-1}K^{-1}};\ \alpha_T = 3\times10^{-6}\,\mathrm{K^{-1}};\ K^* = 1{,}54\times10^{2}\,\mathrm{Ws};\ s_v = 2\mathrm{ms^{-1}};$$

$$D_E = 2{,}5\times10^{-3}\,\mathrm{m^2s^{-1}};\ H_0 = 10^{8}\,\mathrm{Col\cdot cm^{-1}s^{-1}};,$$

$$\mu_0 = 4\pi\times10^{-7}\,\mathrm{Hm^{-1}};\ \sigma_0 = 9{,}36\times10^{5}\,\mathrm{Col^2C^{-1}m^{-1}s^{-1}}.$$

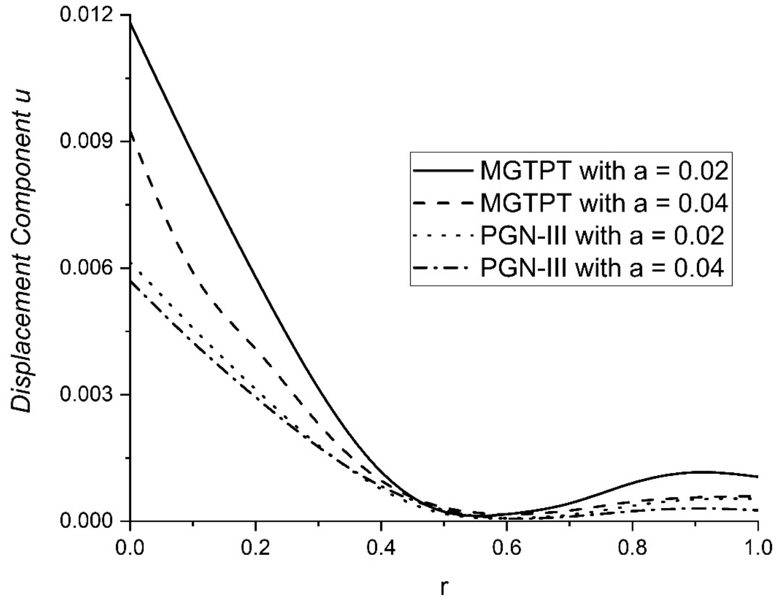

Fig. 2. The radial displacement deviation with two temperature.

Fig. 2 shows how radial displacement u changes under different temperatures for both the MGTPT and PGN-III theories. Radial displacement is observed to be minimum in the MGTPT theory when temperatures do not vary. However, as the value of the two temperature factors increases, the radial displacement in the MGTPT theory also increases. Similarly, the PGN-III theories exhibit a larger variance in the radial displacement, regardless of the presence or absence of two temperatures. Furthermore, it has been observed that as the radial distance increases, the radial displacement decreases. According to Fig. 3, both the MGTPT and PGN-III theories are significantly affected by temperature variance. A higher temperature distribution can be observed in the inner core of the cylinder than in its outer core. Additionally, the presence of two temperatures leads to a higher dispersion of temperature throughout the system.

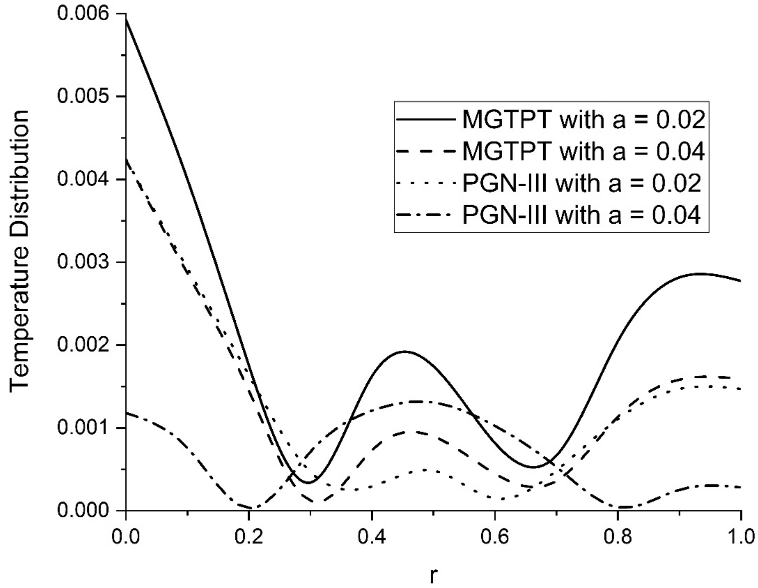

Fig. 3. The temperature deviation with two temperature under various models.

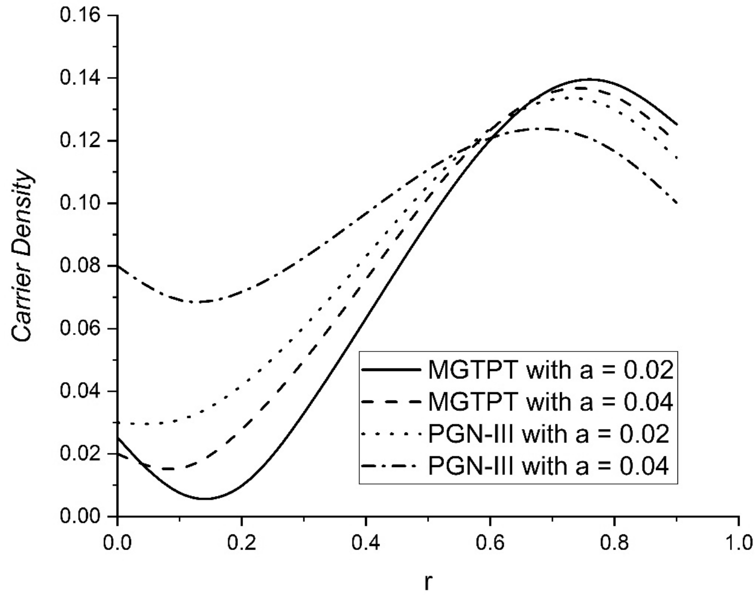

Fig. 4. The deviation in carrier density with two temperature under various models.

Fig. 4 illustrates the variation in carrier density for the MGTPT and PGN-III theories at two different temperatures. Interestingly, it has been observed that the PGN-III theory displays a lower level of fluctuation in carrier density compared to the MGTPT theory when there are no variations in temperature. Surprisingly, the PGN-III theory exhibits the highest level of variance in carrier density overall. Moreover, as the radial distance r increases, there is a significant reduction in the variance of carrier density for both theories. In Fig. 5 to Fig. 7, the fluctuation in stress components for the MGTPT and PGN-III theories under two different temperatures is depicted. It is worth noting that the MGTPT theory generally shows less variance in stress components compared to the PGN-III theory in the absence of temperature variations. However, with an increase in the values of the two temperatures, there is a noticeable rise in the stress components for both theories. Similar to the carrier density, as the radial distance r grows, there is a substantial decrease in the variation of stress components for both the MGTPT and PGN-III theories.

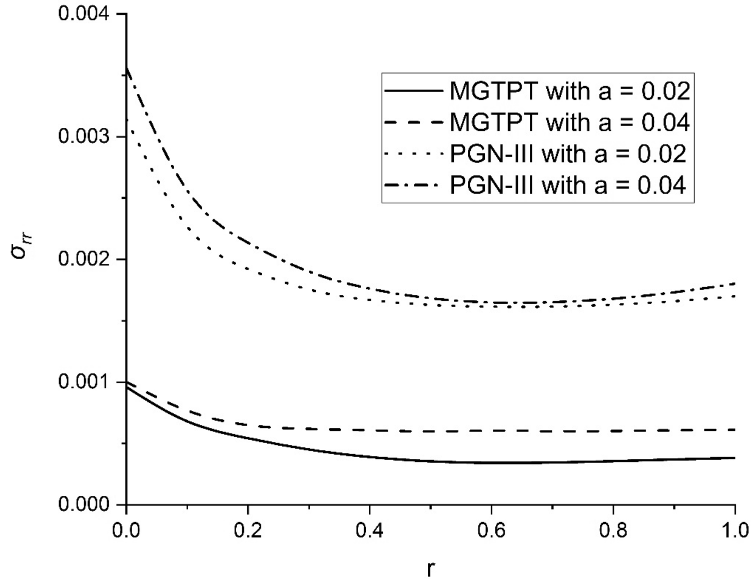

Fig. 5. The variation in radial stress with two temperature for various models.

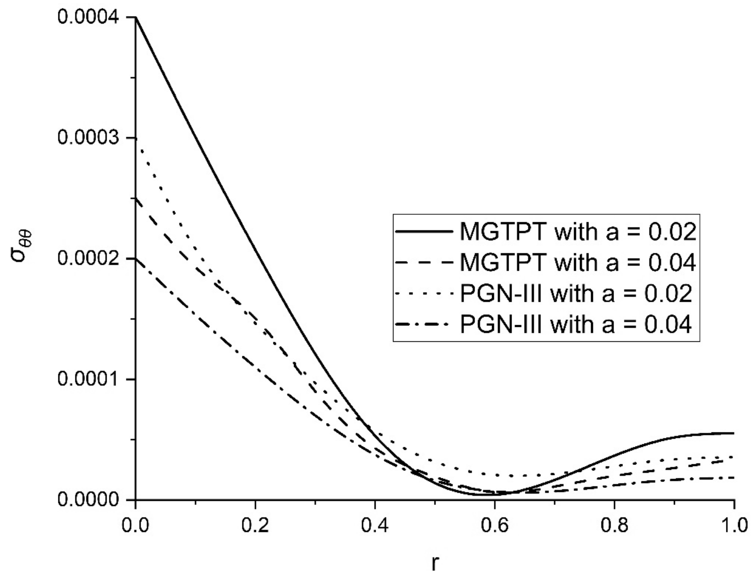

Fig. 6. The variation in hoop stress with two temperature for various models.

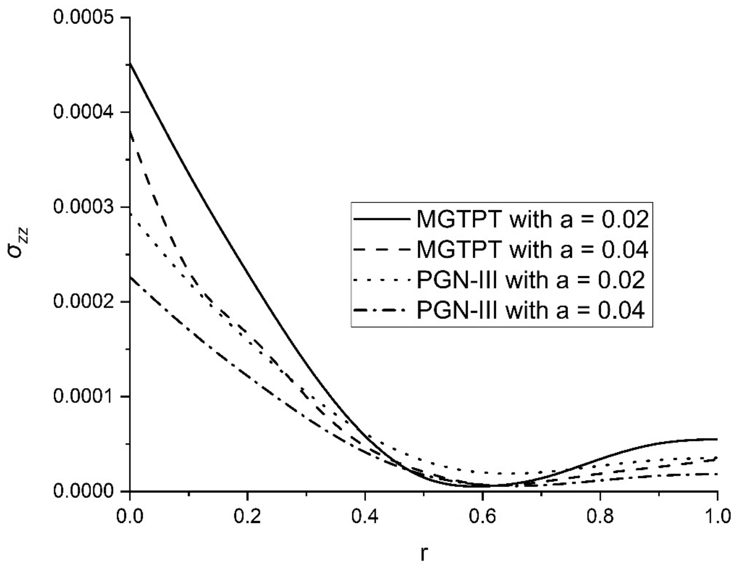

Fig. 7. Deviation in the vertical stress for various models with two temperature.

8. Conclusions.

- The study introduces several photo-thermoelasticity models, with a focus on the MGTPT model. Additionally, the GN-III model is included in the investigation to provide a comprehensive analysis. In order to address the limitations of previous models, the generalized MGTPT model is utilized to explore the physical implications in depth. The study specifically explores the impact of two temperatures on an infinite semiconducting solid cylinder.
- The governing equations have been formulated through the application of the MGTPT framework, which takes into account the presence of two temperature variables in the analysis.
- Various thermoelastic theories with dual temperatures are illustrated graphically to show-case their impact on displacement components, thermal stresses, carrier density, and temperature fields. The graphs clearly indicate that the presence of two temperatures plays a crucial role in the analyzed domains. The thermal effect is observed when semiconductor materials are subjected to concentrated laser or sunlight beams, resulting in vibrations due to the increase in temperature. As a result of their unique properties and performance characteristics, semiconductor materials find wide uses in renewable energy, mainly in solar cells.
- Photothermal techniques offer a fundamental and dependable approach that can provide valuable insights into the de-excitation of materials and the absorption of light. Physicists, geophysicists, thermal engineers, and material designers can all benefit from the concepts elucidated in this paper. Photo-thermoelasticity and thermodynamic challenges can be addressed using the methodology applied in this study.

Nomenclature

δ_{ij}	Kronecker delta,	δ_n	Electronic deformation coefficient,
e_{ij}	Strain tensors(mm^{-1}),	C_E	Specific heat at constant strain,
τ	Photo-generated carrier lifetime,	K_{ij}^*	Materialistic constant,
D_E	Carrier diffusion coefficients,	e_{kk}	Cubical dilatation,
N_0	Carrier concentration at equilibrium position,	κ	Coupling parameter for thermal activation,

λ, μ	Lame's elastic constants,	T_0	Reference temperature s.t. $\left\|T / T_0\right\| << 1$,
β_{ij}	Thermal elastic coupling tensor,	t	Time,
ρ	Medium density (Kgm^{-3}),	Ω	Angular frequency,
ϵ_{ijk}	Permutation symbol,	a_{ij}	Two temperature parameter,
u_i	Components of displacement(m),	φ	Conductive temperature,
α_t	Linear thermal expansion coefficient,	τ_0	Thermal relaxation parameter,
N	Carrier density,	E_g	Energy gap of the semiconductor parameter,
K_{ij}	Coefficient of Thermal conductivity,	d_n	Coefficient of electronic deformation,
T	Thermodynamic temperature,	σ_{ij}	Stress tensors (Nm^{-2}),
s_v	Surface recombination velocity		

РЕЗЮМЕ. Напівпровідний циліндр, який обертається, досліджено в рамках фототермопружності. На циліндр діє експоненціальний імпульс, що моделюється як змінний тепловий потік. Використовуються фототеплові рівняння теплопередачі Мура-Гібсона-Томпсона. Вони включають дві температури для опису основних рівнянь системи. Використовується перетворення Лапласа, що дозволяє отримати більш ефективний та точний розв'язок. Для розрахунку компонентів зміщення, густини носіїв температури, теплових напружень і температуропровідності у фізичній області використовуються методи чисельної інверсії. Крім того, програмне забезпечення MATLAB використовується для створення графічних зображень усіх параметрів, залучених до дослідження. Ці візуалізації ілюструють вплив теплової релаксації та різних теорій термопружності, які розглядають дві температури.

КЛЮЧОВІ СЛОВА: напівпровідний циліндр, дві температури, модифікований теплообмін Мура-Гібсона-Томпсона, експоненціальний імпульс.

References.

1. *Duhamel J.M.*: Memories of the molecular actions developed by changes in temperatures in solids. Mummy Div. Sav. (AcadSci Par.). 5, 440 – 498 (1938).
2. *Biot M.A.*: Thermoelasticity and Irreversible Thermodynamics. J. Appl. Phys. 27, 240 – 253 (1956). https://doi.org/10.1063/1.1722351.
3. *Cattaneo C.*: A form of heat-conduction equations which eliminates the paradox of instantaneous propagation. Comptes Rendus, Acad. Sci. Paris, Ser. II. 247, 431 – 433 (1958).
4. *Vernotte P.*: Les paradoxes de la theorie continue de l'equation de lachaleur. Comptes Rendus, Acad. Sci. Paris, Ser. II. 246, 3154 – 3155 (1958).
5. *Vernotte P.*: Some possible complications in the phenomena of thermal conduction. Comptes Rendus, Acad. Sci. Paris, Ser. II. 252, 2190 – 2191 (1961).
6. *Lord H.W., Shulman Y.*: A generalized dynamical theory of thermoelasticity. J. Mech. Phys. Solids. 15, 299 – 309 (1967). https://doi.org/10.1016/0022-5096(67)90024-5.
7. *Chen P.J., Gurtin M.E.*: On a theory of heat conduction involving two temperatures. Zeitschrift für Angew. Math. und Phys. ZAMP. 19, 614 – 627 (1968). https://doi.org/10.1007/BF01594969.
8. *Green A.E., Lindsay K.A.*: Thermoelasticity. J. Elast. 2, 1–7 (1972). https://doi.org/10.1007/BF00045689.
9. *Dhaliwal R.S., Sheriff H.H.*: Generalized Thermoelasticity for Anisotropic Media. Q. Appl. Math. 38, 1–8 (1980). https://doi.org/https://doi.org/10.1090/qam/575828.
10. *Green A.E., Naghdi P.M.*: A re-examination of the basic postulates of thermomechanics. Proc. R. Soc. London. Ser. A Math. Phys. Sci. 432, 171 – 194 (1991). https://doi.org/10.1098/rspa.1991.0012.
11. *Green A.E., Naghdi P.M.*: On Undamped Heat Waves In An Elastic Solid. J. Therm. Stress. 15, 253 – 264 (1992). https://doi.org/10.1080/01495739208946136.
12. *Green A.E., Naghdi P.M.*: Thermoelasticity without energy dissipation. J. Elast. 31, 189 – 208 (1993). https://doi.org/10.1007/BF00044969.
13. *Lasiecka I., Wang X.*: Moore-Gibson-Thompson equation with memory, part II: general decay of energy. Anal. PDEs. 1 – 22 (2015). https://doi.org/https://doi.org/10.48550/arXiv.1505.07525.

14. *Quintanilla R.*: Moore – Gibson – Thompson thermoelasticity. Math. Mech. Solids. 24, 4020 – 4031 (2019). https://doi.org/https://doi.org/10.1177/1081286519862007.
15. *Quintanilla R.*: Moore-Gibson-Thompson thermoelasticity with two temperatures. Appl. Eng. Sci. 1, 100006 (2020). https://doi.org/10.1016/j.apples.2020.100006.
16. *Fernández J.R., Quintanilla R.*: Moore-Gibson-Thompson theory for thermoelastic dielectrics. Appl. Math. Mech. 2021 422. 42, 309–316 (2021). https://doi.org/10.1007/S10483-021-2703-9.
17. *Bazarra N., Fernández J.R., Quintanilla R.*: Analysis of a Moore-Gibson-Thompson thermoelastic problem. J. Comput. Appl. Math. 382, 113058 (2021). https://doi.org/10.1016/j.cam.2020.113058.
18. *Kaur I., Singh K., Craciun E.-M.*: A Mathematical Study of a Semiconducting Thermoelastic Rotating Solid Cylinder with Modified Moore–Gibson–Thompson Heat Transfer under the Hall Effect. Mathematics. 10, 2386 (2022). https://doi.org/10.3390/math10142386.
19. *Kaur, I., Lata, P., Singh, K.*: Memory-dependent derivative approach on magneto-thermoelastic https://doi.org/10.1186/s40712-020-00122-2transversely isotropic medium with two temperatures. Int. J. Mech. Mater. Eng. 15, (2020).
20. *Lata P., Kaur I., Singh K.*: Deformation in transversely isotropic thermoelastic thin circular plate due to multi-dual-phase-lag heat transfer and time-harmonic sources. Arab J. Basic Appl. Sci. 27, 259 – 269 (2020). https://doi.org/10.1080/25765299.2020.1781328.
21. *Kaur I., Singh K.*: A Study of Influence of Hall Effect in Semiconducting Spherical Shell with Moore-Gibson-Thompson-Photo-Thermoelastic Model. Iran. J. Sci. Technol. Trans. Mech. Eng. (2022). https://doi.org/10.1007/s40997-022-00532-x.
22. *Kaur I., Singh K.*: Plane wave in non-local semiconducting rotating media with Hall effect and three-phase lag fractional order heat transfer. Int. J. Mech. Mater. Eng. 16, 1 – 16 (2021). https://doi.org/10.1186/S40712-021-00137-3/FIGURES/16.
23. *Kaur I., Singh K.*: Modified Moore–Gibson–Thompson Thermoelastic Model with Hyperbolic Two Temperatures Effect on Semiconducting Thermoelastic Solid Cylinder. Mech. Solids. 58, 1723–1737 (2023). https://doi.org/10.3103/S0025654423600745.
24. *Kaur I., Singh K., Craciun E.-M.*: Moore – Gibson – Thompson Coupled Hygro-Photo-Thermoelastic Solid Cylinder with Hyperbolic Two Temperatures. Mech. Solids. 58, 2197 – 2214 (2023). https://doi.org/10.3103/S0025654423601799.
25. *Singh K., Kaur I., Craciun E.-M.*: Hygro-photo-thermoelastic solid cylinder under moisture and thermal diffusivity with Moore-Gibson-Thompson theory. Discov. Mech. Eng. 2, 21 (2023). https://doi.org/10.1007/s44245-023-00028-1.
26. *Mahdy A.M.S., Lotfy K., Ahmed M.H., El-Bary A., Ismail E.A.*: Electromagnetic Hall current effect and fractional heat order for microtemperature photo-excited semiconductor medium with laser pulses. Results Phys. 17, 103161 (2020). https://doi.org/10.1016/j.rinp.2020.103161.
27. *Abouelregal A.E., Atta D.*: A rigid cylinder of a thermoelastic magnetic semiconductor material based on the generalized Moore – Gibson – Thompson heat equation model. Appl. Phys. A Mater. Sci. Process. 128, 1 – 14 (2022). https://doi.org/10.1007/S00339-021-05240-Y/TABLES/7.
28. *William H. Press, Saul A. Teukolsky, Brian P. Flannery*: Numerical recipes in Fortran. Cambridge University Press, Cambridge (1980).

From the Editorial Board: The article corresponds completely to submitted manuscript.

Надійшла 03.03.2023 Затверджена до друку 16.04.2024